HHS Public Access

Author manuscript

IEEE Trans Biomed Eng. Author manuscript; available in PMC 2017 September 01.

Published in final edited form as:

IEEE Trans Biomed Eng. 2016 September ; 63(9): 1787–1794. doi:10.1109/TBME.2016.2591924.

Electrophysiological Source Imaging of Brain Networks Perturbed by Low-intensity Transcranial Focused Ultrasound

Kai Yu [Student Member, IEEE],
Department of Biomedical Engineering, University of Minnesota

Abbas Sohrabpour [Student Member, IEEE], and
Department of Biomedical Engineering, University of Minnesota

Bin He [Fellow, IEEE]
Department of Biomedical Engineering and the Institute for Engineering in Medicine, University of Minnesota, Minneapolis, MN 55455 USA

Abstract

Objective—Transcranial focused ultrasound (tFUS) has been introduced as a noninvasive neuromodulation technique with good spatial selectivity. We report an experimental investigation to detect noninvasive electrophysiological response induced by low-intensity tFUS in an *in vivo* animal model, and perform electrophysiological source imaging (ESI) of tFUS-induced brain activity from noninvasive scalp EEG recordings.

Methods—A single ultrasound transducer was used to generate low-intensity tFUS (I_{spta}<1 mW/cm^2) and induce brain activation at multiple selected sites in an *in vivo* rat model. Up to 16 scalp electrodes were used to record tFUS-induced EEG. Event related potentials (ERPs) were analyzed in time, frequency, and spatial domains. Current source distributions were estimated by ESI to reconstruct spatio-temporal distributions of brain activation induced by tFUS.

Results—Neuronal activation was observed following low-intensity tFUS, as correlated to tFUS intensity and sonication duration. ESI revealed initial focal activation in cortical area corresponding to tFUS stimulation site, and the activation propagating to surrounding areas over time.

Conclusion—The present results demonstrate the feasibility of noninvasively recording brain electrophysiological response in vivo following low-intensity tFUS stimulation, and the feasibility of imaging spatio-temporal distributions of brain activation as induced by tFUS in vivo.

Significance—The present approach may lead to a new means of imaging brain activity using tFUS perturbation and a closed-loop ESI-guided tFUS neuromodulation modality.

Index Terms

transcranial focused ultrasound (tFUS); EEG source imaging; in vivo animal model; perturbation-based neuroimaging

Correspondence to: Bin He.

I. Introduction

Brain activity is distributed over the 3-dimensional space and evolves in time. It is of great importance to be able to image noninvasively brain dynamics and connectomics with high spatial and temporal resolution [1, 2]. Perturbation-based neuroimaging methods [2, 39] combining the light-based, or electrical/electromagnetic neuromodulations with a variety of neuroimaging modalities, like electroencephalography (EEG), functional magnetic resonance imaging (fMRI) and magnetoencephalography (MEG), are valuable tools for understanding the brain networks. Optogenetic neuromodulation, a light-based neuromodulation method, demonstrates excellent spatiotemporal specificity but requires an invasive implantation procedure [3]. Electrical/electromagnetic-based methods, such as the deep brain stimulation (DBS) [4, 40], vagus nerve stimulation (VNS) [5], electro-convulsive therapy (ECT) [6], transcranial magnetic stimulation (TMS) [7, 39], transcranial direct current stimulation (tDCS) [8, 41] and transcranial alternating current stimulation (tACS) [9] have been pursued to modulate local neural circuits, or treat various neurological and mental disorders. Compared to DBS and VNS, TMS and tDCS/tACS have the merit of being non-invasive, but have limited spatial resolution and focality.

Recently, transcranial focused ultrasound (tFUS) has been pursued for non-invasive neuromodulation due to its high spatial resolution [10-12]. In vivo experiments (in animals) have been reported using a range of ultrasonic parameters achieving either activation or suppression of neural activity. Yoo et al [13] used a rabbit model to demonstrate that tFUS with a fundamental frequency of 690 kHz and spatial-peak temporal-average intensity (I_{spta}) of 6.3 W/cm^2 excites the exposed motor cortex, leading to behavioral manifests such as movement and detectable changes in the recorded electromyography (EMG) signals from subdermal electrodes inserted into forelimb muscle. Blood-oxygen-level dependent (BOLD) signals were already observed through fMRI studies using a lower ultrasound intensity (I_{spta}) of 1.6 W/cm^2, whereas the acoustic stimulation with a spatial-peak pulse-average intensity (I_{sppa}) of 6.4 W/cm^2 lasting for over 7-8 s renders a reduction in the magnitude of the P30 visual evoked potential (VEP). Low-intensity tFUS (I_{spta}: 300 mW/cm^2) was used by Yoo et al [14] to sonicate the thalamus of anesthetized rats, and as indicated through physiological and behavioral changes, the rats' recovery time was shortened significantly as measured by voluntary movement and pinch response. Using another low-intensity ultrasound stimulation experiment (I_{spta}: less than 13.5±3.8 mW/cm^2, fundamental frequency: 320 kHz), Deffieux et al [15] administered tFUS to the left frontal eye field (FEF) in two awake macaque rhesus monkeys, and found that tFUS delayed the ipsilateral mean antisaccade (AS) latencies compared to the non-sonication case. Most recently, Lee et al [16] targeted the 250 kHz tFUS at the primary sensorimotor cortex and visual cortex of anesthetized sheep, and recorded tFUS-evoked electrophysiological signals using a bilateral EMG and 2-channel subdermal EEG system. It was found that the ultrasound intensity I_{sppa} needed to be greater than 6 W/cm^2 to elicit motor evoked potentials (MEPs) and sonication-triggered visual evoked potentials (sVEPs). Minor micro-hemorrhages in the primary visual cortex were reported which were due to the use of high intensity tFUS, indicating that the ultrasound parameters need to be considered carefully to ensure safe neuromodulatory effects.

In the past years, several groups have applied ultrasound neuromodulation in humans. Hameroff et al [17] harnessed a commercially available ultrasound machine working in standard B-mode to dose chronic pain subjects with transcranial ultrasound (I_{spta}: 152 mW/cm^2 at transducer), and they reported that the subjects' mood were improved for 10 minutes after the ultrasound mediation. Legon et al [18] examined the effect of pulsed ultrasound stimulation on peripheral somatosensory circuits by stimulating fingertips. Two ultrasound stimulation waveforms were designed to evoke either mechanical sensation (I_{spta}: 11.8 W/cm^2) or thermal sensation (I_{spta}: 54.8 W/cm^2), and the sonication effects on the neural circuits were indicated by both EEG and fMRI. Later, the group further examined the tFUS (I_{sppa}: 23.87 W/cm^2 at scalp) on sensory-evoked potentials through concurrent EEG recordings [11]. Median nerve stimulations were introduced in this study when the tFUS was administered to the scalp region over the somatosensory cortex. Their EEG recordings showed that tFUS attenuated the amplitudes of the somatosensory evoked potentials, and modulated the spectral content of sensory-evoked brain oscillations. Mueller et al [19] researched the ultrasound-modulatory effect on the EEG phase dynamics of the somatosensory cortex from four-channel EEG recordings. The tFUS (I_{sppa}: 23.87 W/cm^2) altered the phase distribution of intrinsic brain activity in beta-band frequencies, and modulated the phase rate of beta and gamma frequencies. Lee et al [20] reported their recent human study, in which tFUS (I_{spta}: 1.5 W/cm^2 at transducer, 350 mW/cm^2 behind the skull) was delivered to the hand region of the somatosensory cortex, using subjects' individual anatomical MR images to guide the transducer over the desired region on the cortex. The participating subjects reported the experienced tactile sensations whilst tFUS stimulations were administered. Two-channel EEG recordings from the primary somatosensory cortex revealed that tFUS stimulations were capable of evoking potentials in the hand region of the primary somatosensory cortex, consistent with the subjects' reports (of sensation in the hand).

In the present study, we test the hypothesis whether low-intensity tFUS (e.g., $I_{spta} < 1$ mW/cm^2) can be used as a controlled perturbation to initiate neural activation. We further use electrophysiological source imaging based on multi-channel scalp EEG recordings to image tFUS induced brain activation in an attempt to perturb specific nodes within a brain network under study to determine the role each node plays within the network. The initial results were reported in the BRAIN Investigators Meeting held in December 2015 [21].

II. Experimental Design and Setup

A. Sonication Setup

tFUS pulses were produced in a burst mode by a single-element focused ultrasound transducer (V389, Olympus, USA) and were employed to perturb the intact rat brain in anesthesia, as shown in Fig. 1. This ultrasound transducer has a diameter of 38.1 mm, a center frequency of 500 kHz, a -6 dB bandwidth of 300-690 kHz and a nominal focal distance of 55 mm. The transducer is controlled by two function generators (33220A, Keysight Technologies, USA) that manage the time sequence of ultrasonic output, so as to produce a specified time burst of pulses with 2 kHz pulse repetition frequency (PRF) in 3 s inter-sonication intervals. Such ultrasound temporal protocol was developed following Tufail

et al. [22, 23] and Yoo et al. [13, 16]. Instead of tone burst mode (i.e. tens of cycles in each pulse duration) used in their experiments, in this present study we used the single-pulse burst mode as shown in Fig.1 to significantly reduce the I_{spta} and I_{sppa}. These pulses triggered an ultrasonic pulser unit (5077PR, Olympus NDT, USA), which controlled the voltage amplitudes fed into the transducer. To guide the ultrasound energy onto a certain brain location, a customized conical ultrasound collimator was fabricated using a polypropylene funnel and a polytetrafluoroethylene cylindrical tube, and was then filled with ultrasound coupling gel (Aquasonic 100 Ultrasound Transmission Gel, Parker Laboratories, USA). This collimator had an inner diameter of 1.7 mm at its tip, and its total length equaled the focal distance of the transducer. The directed acoustic intensities (I_{spta}: 0.1-0.6 mW/cm^2, I_{sppa}: 0.74-4.6 mW/cm^2, spatial-peak temporal-peak intensity I_{sptp}: 38-252 mW/cm^2, corresponding to spatial peak rarefactional pressure P_r amplitude of 18.3-45.9 kPa) transported through the collimator were then measured using a calibrated hydrophone (HNR500, Onda, USA) placed behind a piece of freshly excised Wistar rat skull. To measure such ultra-low intensity, a calibrated, broadband hydrophone preamplifier (AH-2010-025, Onda, USA) was also employed. Notably, the administered ultrasound intensities were far less than the safety limit, i.e. I_{spta} of 720 mW/cm^2 and I_{sppa} of 190 W/cm^2, used in ultrasound diagnostic imaging systems, set forth by the U.S. Food and Drug Administration (FDA) [24]. By further measuring the acoustic pressure directly at the tip of the collimator, the ultrasound insertion loss as calculated for the pressure, was approximately -14 dB across the sites on the skull where the transducer would be placed in our experiment. The collimator, the skull sample and the needle hydrophone were aligned using a 3-axis positioning stage. This positioning stage was controlled by a stepper motor system, and was also used to aim the ultrasound transducer and collimator to a specific scalp region during the in vivo experiments.

B. In Vivo Rat Model

The Wistar rat was chosen for the in vivo study mainly due to its relatively big cranial size and thinner skull among the rat species. Three one-year-old rat subjects were used, and each was anesthetized using katamine/xylazine mixture (75 mg/kg and 10 mg/kg respectively) with certain dosage determined by both the rat's weight and the anesthetic duration (2-3 hours). The hair over the rat's scalp, the nape, hind limbs and caudal regions were carefully removed using an electric hair trimmer and a hair remover cream lotion, to expose the skin. After the exposed skin was further degreased using alcoholic pads, and the impedance was lowered using skin prep gel, EEG and ECG electrodes were then attached to the treated skin regions, accordingly. During the experiment, a rectal thermometer and a heating lamp were used to monitor and maintain the rat body temperature. This experiment protocol was approved by the University of Minnesota Institutional Animal Care and Use Committee.

C. Electrophysiological Signal Detection and Preprocessing

All the electrophysiological signals were acquired, amplified, filtered and digitized using a multi-channel NeuroScan system (Synamps 2, Compumedics, USA) with a sampling rate of 1 kHz. The EEG was simultaneously recorded and synchronized with the ultrasound system so as to know exactly when the sonication pulses were administered. During the data acquisition, the bandpass filters with respective cutoff frequencies were applied to EEG, and

ECG channels. 8-channel EEG recordings were used to assess the effect of sonication intensity on brain activation, and 16-channel EEG recordings were used to measure the spatiotemporal distribution of the brain electrical activity as induced by tFUS. EEG data were further bandpass filtered and preprocessed for source imaging analysis. The epochs of ultrasonic stimulations were aligned by using the event markers transmitted by the function generator in the sonication setup. Additionally, the short-time Fourier transform (STFT) of the mean global field power (MGFP) of the averaged ERP was also plotted using a Hamming window of length 32 ms and overlap of 4 ms.

A sham condition was designed by removing the ultrasound collimator and turning the transducer away from the rat scalp while transmitting ultrasound pulses. In order to only image the brain activity due to sonication and to reduce the effect of common activity perceived in the sham condition, the common components of activity observed in the sham condition were removed from the ERP signals prior to source imaging. Auditory pathways may be activated during the ultrasound pulse generation, as animals like rat are capable of hearing frequency ranges much higher than human beings [25]. This was achieved by performing the principal component analysis (PCA) and identifying components demonstrating a high correlation with the sham components. Independent component analysis (ICA) [37] can be used to perform this analysis, as well. ICA is a promising method when dealing with artefacts, since such interferences are independent of the brain activity and ICA is efficient in detecting and removing those signals. Mainly the interferences can be roughly categorized as physiological artefacts such as eye movement, muscle contraction, and electromagnetic interferences from stimulation or 60 Hz power-line noise. In our experiment the animals were anesthetized, the aforementioned physiological artefacts were minimal and absent after averaging. Since ultrasound stimulation was administered, no electromagnetic interference was introduced by stimulation and power-line noise was removed with a 60-Hz notch filter. The PCA [38], however, determines main components in the data based on their strength (signal energy which is related to signal's second norm). Thus we could compare strong components present in the two conditions, i.e. sham vs. stimulation, to reject common components which are related to background brain processes (not artefacts). For example, auditory pathways may be activated during the ultrasound pulse generation, as animals like rats are capable of hearing frequency ranges much higher than human beings. In this sense, ICA might not add an extra value for component analysis, thus PCA and ICA could be used interchangeably and both analyses actually show many similar components.

D. EEG Source Imaging

We used a publicly available Wistar rat MRI atlas (http://www.idac.tohoku.ac.jp/bir/en/db/rb/101028.html) to build a generic boundary element method (BEM) model of the rat head, as individual head MRI was not available at the time [26]. The BEM head model consisted of three layers of tissue, namely, the skin, the skull and the brain with conductivities of 0.33 S/m, 0.0165 S/m and 0.33 S/m, respectively [27-29]. The minimum norm (MN) algorithm [30] was used to solve the inverse problem. As mentioned previously using PCA, the components of the EEG signal that were highly correlated with the EEG recorded during the sham condition were removed from the EEG

prior to source analysis. The source imaging was performed for the duration of the sonication and after cessation of stimulation, for about several hundreds of milliseconds.

E. Statistical Testing

In order to test the significance of the results when comparing ERP signals to the sham condition, we performed statistical testing to determine time intervals at which the ERP signals and the sham condition were significantly different ($p<0.025$). We performed a paired t-test to this end. The data recorded at different channels of the EEG were treated as samples drawn from the two conditions (sham vs. ERP induced by sonication). The amplitudes of the signal in the two conditions were compared over time to find time intervals at which a significance of ($p<0.025$) was achieved [11, 20, 31].

III. Results

A. tFUS-evoked Brain Activities

Fig. 2 shows the 8-channel scalp EEG recordings of the tFUS-evoked brain activities in a rat from three ultrasound intensities (as listed in Table I) used to sonicate the targeted right anterior cortex. These intensities are due to three different excitation voltages that drive the transducer. After averaging across 300 trials, the results are illustrated in the time course (from -200 to 600 ms, 0 ms indicates the onset of the 200-ms sonication) both with butterfly plots and MGFP plots. Fig. 2 indicates that even when a low-intensity sonication (I_{spta}: 0.1 mW/cm^2, I_{sppa}: 0.7 mW/cm^2) is administered with the applied ultrasound pressure recorded in Fig. 2(b), the rat brain shows an observable time-locked activation as perceivable in the EEG. When increasing the input ultrasound intensities, the recorded EEG shows increasing response amplitudes and extended activations as depicted in Figs. 2(a) and (c). If one takes the time integral of the MGFP within the sonication duration of 200 ms, the results demonstrate an increasing trend shown in Fig. 2(d). These integral values are calculated using trapezoidal integration method with an integration step of 1 ms.

Fig. 3 shows 16-channel scalp ERPs averaged from 600 trials of another rat subject. The channels indicated by the orange squares, i.e. electrode #9, #12, and #16 are further magnified in Fig. 3(d), in which the neural recording under three sonication durations are plotted for each electrode. Within sonication period, all those three conditions use acoustic intensity I_{spta} of 0.6 mW/cm^2 (I_{sppa}: 4.6 mW/cm^2, I_{sptp}: 252 mW/cm^2) when the tFUS wave reaches the skull covering the targeted cortical region. The vertical dotted lines in Fig. 3(d) show the time points of interest at the extrema of neural activity time course. Fig. 3(e) depicts the averaged signal values and standard deviations at the four time points (i.e. 17, 35, 95 and 294 ms) read from the three individual EEG electrodes (indicated by orange squares in Fig. 3(a)(b)(c)). Significant differences exist at 294 ms among three sonication durations from recorded signals by three electrodes. Electrodes #12 and #16 also present significant differences at 35 ms in the signal profiles by the 5-ms and 200-ms sonication durations.

Inevitably, the audible sound from tFUS may also result in auditory evoked potentials. In the in vivo experiment, during the sham condition, the transducer keeps transmitting ultrasound as in the stimulation session, using 200 ms sonication, while the transducer is flipped to

point away from the animal. Fig. 4(a) depicts the MGFP values of the 16-channel EEG recordings of the sham ultrasound condition (red), and its comparison to the 200 ms tFUS condition (black). The gray vertical bars at 8-19 ms, 33-109 ms, and 267-311 ms indicate significant differences (paired t-test, $p<0.025$) in the amplitude of evoked neural signals between the sham and the transcranial sonication conditions. Fig. 4(b) shows the time-frequency plots depicting the spectral contents in α (7-12 Hz), β (13-30 Hz), and lower γ (31-55 Hz) frequency bands of the elicited brain activity after the onset (dashed vertical lines) of the sonication. Compared to the sham condition, we also found significant differences existing within each frequency band during 0-100 ms and 200-250 ms produced by the 200 ms tFUS. Hence, based on the analyses of global field power and spectral power, the tFUS-evoked brain activities can be distinguished from the sham condition.

B. tFUS-EEG Source Imaging

Signals from the sham condition have been subtracted from the recordings with the tFUS condition. Solving the inverse problem using the MN method, the EEG source images were obtained to estimate the spatial location of the ultrasound perturbation and its induced brain activation. In the presented ESI results, we found that the estimated source covered cortical regions including the targeted region of the ultrasound beam. Further, a series of EEG topographic voltage maps and source images at several time points of relative signal peaks (21, 50, 109 ms) in the MGFP plot are depicted in Fig. 5(c), (d) and (e), while the relative locations of the rat brain, the cranial bone, the ultrasound incidence, and the EEG electrodes are shown in Fig. 5(a) and (b), respectively. From the presented source images (Fig. 5(e)), the location of the initial activation (21 ms) aligns with the ultrasound targeting region, and this activation soon propagates to the surrounding cortical regions (50 ms). Because the tFUS keeps depositing mechanical energy during the sonication period, the brain activation source stays at the right anterior cortical region (50 and 109 ms), and meanwhile several other cortical areas become active successively.

When the same ultrasound beam is directed at another anterior cortical region which is more lateral, the ultrasound intensity reaching the brain tissue would be even less due to an increasing skull thickness of the rat cranium. Therefore, the amplitudes decrease as observed in the topographic voltage maps and the EEG source imaging results (Fig. 6(d) and (e)). From these results, it is shown once more that the initiation region of cortical activation (17 ms) follows the ultrasound incidence site, and later at 68 ms, this source activation propagates to other brain regions while the initiation region remains being activated by the ongoing ultrasound stimulation.

A third rat was also studied using the same sonication condition as harnessed in Figs. 5-6, whereas ultrasound incidence site was changed to the location of electrode #9 as mapped in Fig. 3(a). Similar ESI results were observed in this case comparable to other two animals (data not shown).

IV. Discussion

We have conducted an experimental investigation to demonstrate the feasibility of noninvasively recording brain electrical activity as induced by low-intensity tFUS in an in

vivo animal model. We have also demonstrated, for the first time, that it is possible to image brain electrical activity from noninvasive scalp EEG recordings following tFUS perturbation. Our results suggest that ESI may become a useful tool to derive biomarkers to quantify tFUS effects and guide its use for neuromodulation. Such noninvasive biomarker, while obtained in real time, may offer important insights to optimize tFUS stimulation parameters and make tFUS a closed-loop neuromodulation modality.

Our work also suggests using tFUS as an important guide for perturbation based neuroimaging. In perturbation based neuroimaging [2, 39], external energy is applied to alter the neural information processing; the spatio-temporal activation patterns as altered due to such perturbations, can then be used to identify and delineate the mechanisms of neural activation and pathology. For this purpose, it is important to use low intensity neuromodulation so the injected energy will only present perturbations to avoid global and wide-spread effects.

In our work, using a single-element focused ultrasound transducer with a collimator, we introduced the low-intensity tFUS (I_{spta} as low as 0.1 mW/cm^2, and I_{sppa} as low as 0.7 mW/cm^2) as a brain perturbation tool and demonstrated the capability of noninvasively recording electrophysiological responses of the brain following such low-intensity tFUS perturbation. By stimulating multiple sites and localizing the initiation site of the induced activity, our results confirmed such local activation can be noninvasively recorded and localized to the target site (corresponding to tFUS beam) by means of ESI.

Considering the different skull thicknesses in various in vivo animal models or human subjects, one may need to compare the ultrasound intensities at the brain tissue (as opposed to ultrasound pressure at the scalp). In our in vivo rat experiment for tFUS-ESI, the applied I_{spta} (0.1-0.6 mW/cm^2) is much lower than the lowest ultrasound spatial-peak temporal-average intensity (13.5±3.8 mW/cm^2) ever reported in the past in vivo studies [15], to the best of our knowledge. For the neuroimaging purpose, such ultra-low intensity tFUS shall not damage the brain, but is still able to perturb the brain network. The present experiment has identified a low but effective tFUS intensity for EEG source imaging. Additionally, the ultrasound spatial-peak temporal-average intensity of less than 1 mW/cm^2 (at the tip of collimator) ensures the non-invasive merit of tFUS (such level of stimulation did not induce other physiological activities such as leg movement, as the EMG did not show any detectable signal at both hind limbs). However, these parameters (at the tip of collimator and at the cortex) would need to be modified and scaled up, if to be used for human experiments.

In our experiment, the fundamental ultrasound frequency used was 500 kHz, which may not be an optimal choice in terms of eliciting behavioral changes and neuromodulation. Some previous studies aiming to study effective ultrasound parameters, to maximize sensorimotor responses in rats, reported that frequencies lower than 500 kHz were more effective in eliciting stronger EMG responses [32]. However, as lower frequencies lead to poorer ultrasound spatial specificity, a trade-off between the stimulating efficiency and spatial focality exists. Further investigation on effective frequencies needs to be done on an application-specific manner, as effective frequencies that elicit maximal behavioral responses, might be different for different networks in the brain.

Our results, in general, support the hypothesis that tFUS-induced brain activity is generated from the point of cortex targeted by the ultrasound beam and propagates to surrounding tissue. Since the ultrasound transducer was not targeted at a specific location of cortex, and low intensity ultrasound (I_{spta}<1 mW/cm^2) was used in the in vivo rat experiment, no behavioral change was observed. Our results indicate a focus of activity forming under the ultrasound collimator on the cortex and its later propagation to nearby tissue. This is the first evidence of ultrasound-induced electrical activity captured non-invasively by dynamic EEG source imaging in a living system, to the best of our knowledge.

While tFUS has been used in recent years to modulate and study the brain [11, 17, 20, 23] the neural effect induced by tFUS remains unclear [33, 34]. Use of ESI represents an opportunity to delineate the mechanism of tFUS by noninvasively mapping the spatio-temporal patterns of brain activation induced by tFUS. The specificity of tFUS and its ability to form concentrated foci, makes the combination of tFUS and ESI an ideal tool for noninvasively studying the brain. Using ESI to monitor the effects of tFUS stimulation can help not only in determining the nature of neuromodulation therapies performed by ultrasound, but also to be used to study normal brain networks by exciting or inhibiting different brain locations [13], i.e. network nodes. Another impact of using ESI technique in ultrasound neuromodulation is that ESI is able to non-invasively document the targeted brain region by the transducer, which is considered as one of the challenges for ultrasound neuromodulation research.

Ultrasound has also been used to treat pathological brain conditions. An early study by Manlapaz et al. [35] on a feline model provided experimental evidence as to the efficacy of ultrasound-induced attenuation of seizure activity and consequently decreased morbidity. A relatively high acoustic intensity of 840 W/cm^2 with a fundamental acoustic frequency of 2.7 MHz was used in the aforementioned study. More recently Min et al. [36] reported on a rat model having pentylenetetrazol-induced epileptic activity; the sonication (I_{spta}: 130 mW/cm^2) was shown to be successful in suppressing the occurrence of epileptic EEG bursts as observed in subdermal two-channel EEG recordings. These in vivo studies show the value of tFUS as a neuromodulation tool. Combined with ESI, the target to be stimulated by tFUS can be determined from electrophysiological recordings, thus allowing precision neuromodulation by assessing the tFUS effects. After tFUS is administered, the pathological activity, e.g. seizure, can be monitored by ESI to study the prognosis of stimulation and treatment efficacy.

While the EEG was used to record and image brain activity as induced by tFUS in the present study, it is anticipated that one can use magnetoencephalography (MEG) [30] to record and image brain activity induced by tFUS. Such demonstration shall be interesting for further investigation, and the present results indicate such possibility [1].

V. Conclusion

In this work, we have demonstrated, in an in vivo experiment in 3 rat subjects, that low-intensity tFUS (e.g. I_{spta} < 1 mW/cm^2) can induce brain electrical activity in the target region of tFUS. We have noninvasively recorded multi-channel scalp EEG following low-

intensity tFUS and have localized and imaged tFUS-induced brain activation from scalp recorded EEG distributions. Our promising results demonstrate the feasibility of noninvasive sensing low-intensity tFUS induced brain activation, and localization and imaging of brain activity from noninvasive scalp EEG signals. The present work suggests that the proposed perturbation based neuroimaging using tFUS-ESI merits further investigation and may become a useful tool for delineating normal and pathological brain networks and circuitry in a well-controlled and noninvasive manner. The ESI guided tFUS may also have important applications to the treatment and management of various brain disorders.

Acknowledgments

The authors would like to thank Dr. Akira Sumiyoshi (Tohoku University, Japan) for sharing their Wistar rat MRI atlas, and Dr. Qi Shao (University of Minnesota) for technical assistance in handling animals.

This work was supported in part by the National Science Foundation under grants CBET-1450956 and CBET-1264782, and by the National Institutes of Health under grants EB014353, EY023101, HL117664, EB021027, and NS096761. K. Yu was partially supported by an MnDRIVE Graduate Research Fellowship from the University of Minnesota.

References

1. He B, Yang L, Wilke C, Yuan H. Electrophysiological Imaging of Brain Activity and Connectivity-Challenges and Opportunities. IEEE Transactions on Biomedical Engineering. Jul.2011 58:1918–1931. [PubMed: 21478071]
2. He B, Coleman T, Genin GM, Glover G, Hu X, Johnson N, et al. Grand challenges in mapping the human brain: nsf workshop report. IEEE Trans Biomed Eng. Nov.2013 60:2983–92. [PubMed: 24108705]
3. LaLumiere RT. A new technique for controlling the brain: Optogenetics and its potential for use in research and the clinic. Brain Stimul. 2011; 4:1–6. [PubMed: 21255749]
4. Lyons MK. Deep brain stimulation: current and future clinical applications. Mayo Clin Proc. 2011; 86:662–672. [PubMed: 21646303]
5. Panescu D. Vagus nerve stimulation for the treatment of depression. IEEE Eng Med Biol Mag. Nov-Dec;2005 24:68–72.
6. Jelovac A, Kolshus E, McLoughlin DM. Relapse following successful electroconvulsive therapy for major depression: a meta-analysis. Neuropsychopharmacology. Nov.2013 38:2467–74. [PubMed: 23774532]
7. Lefaucheur JP, André-Obadia N, Antal A, Ayache SS, Baeken C, Benninger DH, et al. Evidence-based guidelines on the therapeutic use of repetitive transcranial magnetic stimulation (rTMS). Clinical Neurophysiology. 2014; 125:2150–2206. [PubMed: 25034472]
8. Nitsche MA, Paulus W. Excitability changes induced in the human motor cortex by weak transcranial direct current stimulation. J Physiol. Sep 15.2000 527 Pt 3:633–9. [PubMed: 10990547]
9. Kanai R, Chaieb L, Antal A, Walsh V, Paulus W. Frequency-dependent electrical stimulation of the visual cortex. Curr Biol. Dec 9.2008 18:1839–43. [PubMed: 19026538]
10. Kim H, Lee SD, Chiu A, Yoo SS, Park S. Estimation of the spatial profile of neuromodulation and the temporal latency in motor responses induced by focused ultrasound brain stimulation. Neuroreport. May 7.2014 25:475–9. [PubMed: 24384503]
11. Legon W, Sato TF, Opitz A, Mueller J, Barbour A, Williams A, et al. Transcranial focused ultrasound modulates the activity of primary somatosensory cortex in humans. Nat Neurosci. Feb. 2014 17:322–9. [PubMed: 24413698]
12. Mehic E, Xu JM, Caler CJ, Coulson NK, Moritz CT, Mourad PD. Increased anatomical specificity of neuromodulation via modulated focused ultrasound. PLoS One. 2014; 9:e86939. [PubMed: 24504255]

13. Yoo SS, Bystritsky A, Lee JH, Zhang Y, Fischer K, Min BK, et al. Focused ultrasound modulates region-specific brain activity. Neuroimage. Jun 1.2011 56:1267–75. [PubMed: 21354315]
14. Yoo SS, Kim H, Min BK, Franck E, Park S. Transcranial focused ultrasound to the thalamus alters anesthesia time in rats. Neuroreport. Oct 26.2011 22:783–787. [PubMed: 21876461]
15. Deffieux T, Younan Y, Wattiez N, Tanter M, Pouget P, Aubry JF. Low-intensity focused ultrasound modulates monkey visuomotor behavior. Curr Biol. Dec 2.2013 23:2430–3. [PubMed: 24239121]
16. Lee W, Lee SD, Park MY, Foley L, Purcell-Estabrook E, Kim H, et al. Image-Guided Focused Ultrasound-Mediated Regional Brain Stimulation in Sheep. Ultrasound Med Biol. Feb.2016 42:459–70. [PubMed: 26525652]
17. Hameroff S, Trakas M, Duffield C, Annabi E, Gerace MB, Boyle P, et al. Transcranial ultrasound (tus) effects on mental states: a pilot study. Brain Stimul. May.2013 6:409–15. [PubMed: 22664271]
18. Legon W, Rowlands A, Opitz A, Sato TF, Tyler WJ. Pulsed ultrasound differentially stimulates somatosensory circuits in humans as indicated by EEG and FMRI. PLoS One. 2012; 7:e51177. [PubMed: 23226567]
19. Mueller J, Legon W, Opitz A, Sato TF, Tyler WJ. Transcranial Focused Ultrasound Modulates Intrinsic and Evoked EEG Dynamics. Brain Stimul. Sep 6.2014
20. Lee W, Kim H, Jung Y, Song IU, Chung YA, Yoo SS. Image-guided transcranial focused ultrasound stimulates human primary somatosensory cortex. Sci Rep. 2015; 5:8743. [PubMed: 25735418]
21. He, B., Yu, K., Sohrabpour, A., Ebbini, E., Liu, D. BRAIN Initiative Investigators Meeting. Bethesda: 2015. High-resolution multimodal aouctomagnetic neuroimaging of brain activity.
22. Tufail Y, Matyushov A, Baldwin N, Tauchmann ML, Georges J, Yoshihiro A, et al. Transcranial pulsed ultrasound stimulates intact brain circuits. Neuron. Jun 10.2010 66:681–94. [PubMed: 20547127]
23. Tufail Y, Yoshihiro A, Pati S, Li MM, Tyler WJ. Ultrasonic neuromodulation by brain stimulation with transcranial ultrasound. Nat Protoc. Sep.2011 6:1453–70. [PubMed: 21886108]
24. Duck FA. Acoustic saturation and output regulation. Ultrasound in Medicine and Biology. 1999; 25:1009–1018. [PubMed: 10461731]
25. Muller M. Frequency representation in the rat cochlea. Hear Res. Feb.1991 51:247–54. [PubMed: 2032960]
26. Valdes-Hernandez PA, Sumiyoshi A, Nonaka H, Haga R, Aubert-Vasquez E, Ogawa T, et al. An in vivo MRI Template Set for Morphometry, Tissue Segmentation, and fMRI Localization in Rats. Front Neuroinform. 2011; 5:26. [PubMed: 22275894]
27. Oostendorp TF, Delbeke J, Stegeman DF. The conductivity of the human skull: results of in vivo and in vitro measurements. IEEE Trans Biomed Eng. Nov.2000 47:1487–92. [PubMed: 11077742]
28. Lai Y, van Drongelen W, Ding L, Hecox KE, Towle VL, Frim DM, et al. Estimation of in vivo human brain-to-skull conductivity ratio from simultaneous extra- and intra-cranial electrical potential recordings. Clin Neurophysiol. Feb.2005 116:456–65. [PubMed: 15661122]
29. Zhang Y, van Drongelen W, He B. Estimation of in vivo brain-to-skull conductivity ratio in humans. Appl Phys Lett. 2006; 89:223903–2239033. [PubMed: 17492058]
30. Hämäläinen MS, Ilmoniemi RJ. Interpreting magnetic fields of the brain: minimum norm estimates. Medical & Biological Engineering & Computing. 1994; 32:35–42. [PubMed: 8182960]
31. Maris E, Schoffelen JM, Fries P. Nonparametric statistical testing of coherence differences. J Neurosci Methods. Jun 15.2007 163:161–75. [PubMed: 17395267]
32. King RL, Brown JR, Newsome WT, Pauly KB. Effective parameters for ultrasound-induced in vivo neurostimulation. Ultrasound Med Biol. Feb.2013 39:312–31. [PubMed: 23219040]
33. Tyler WJ. Noninvasive Neuromodulation with Ultrasound? A Continuum Mechanics Hypothesis. Neuroscientist. Feb.2011 17:25–36. [PubMed: 20103504]
34. Mueller J, Tyler WJ. A quantitative overview of biophysical forces impinging on neural function. Physical Biology. 2014; 11:051001. [PubMed: 25156965]
35. Manlapaz JS, Astroem KE, Ballantine HT Jr, Lele PP. Effects of Ultrasonic Radiation in Experimental Focal Epilepsy in the Cat. Exp Neurol. Oct.1964 10:345–56. [PubMed: 14211931]

36. Min BK, Bystritsky A, Jung KI, Fischer K, Zhang Y, Maeng LS, et al. Focused ultrasound-mediated suppression of chemically-induced acute epileptic EEG activity. BMC Neurosci. 2011; 12:23. [PubMed: 21375781]

37. Makeig S, Westerfield M, Jung TP, Enghoff S, Townsend J, Courchense E, Sejnowski TJ. Dynamic brain sources of visual evoked responses. Science. 2002; 295:690–694. [PubMed: 11809976]

38. Lagerlund TD, Sharbrough FW, Busacker NE. Spatial filtering of multichannel electroencephalographic recordings through principal component analysis by singular value decomposition. Journal of clinical neurophysiology. 1997; 14:73–82. [PubMed: 9013362]

39. Edelman B, Johnson NJ, Sohrabpour A, Tong S, Thakor N, He B. Systems Neuroengineering: Understanding and Interacting with the Brain. Engineering. 2015; 1:292–308.

40. Johnson MD, Lim HH, Netoff TI, Connolly AT, Johnson N, Roy A, He B. Neuromodulation for brain disorders: challenges and opportunities. IEEE Trans Biomed Eng. 2013; 60:610–624. [PubMed: 23380851]

41. Roy A, Baxter B, He B. High-Definition Transcranial Direct Current Stimulation Induces Both Acute and Persistent Changes in Broadband Cortical Synchronization: A Simultaneous tDCS–EEG Study. IEEE Trans Biomed Eng. 2014; 61:1967–1978. [PubMed: 24956615]

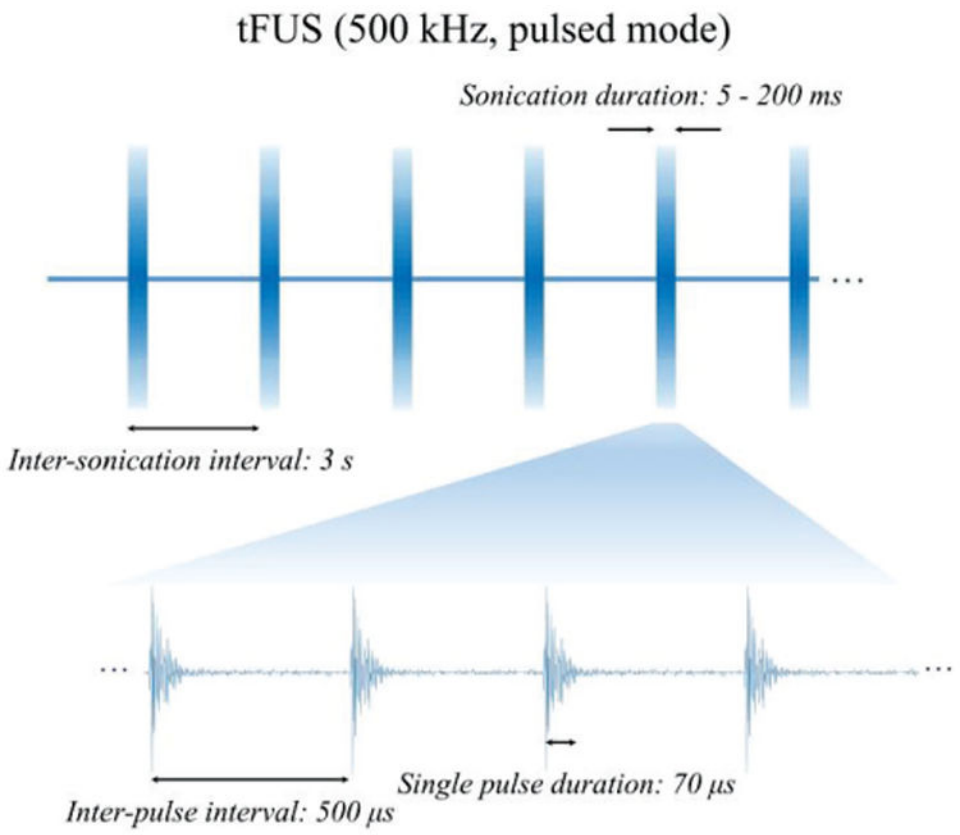

Fig. 1. The sonication waveforms used in the in vivo experiment

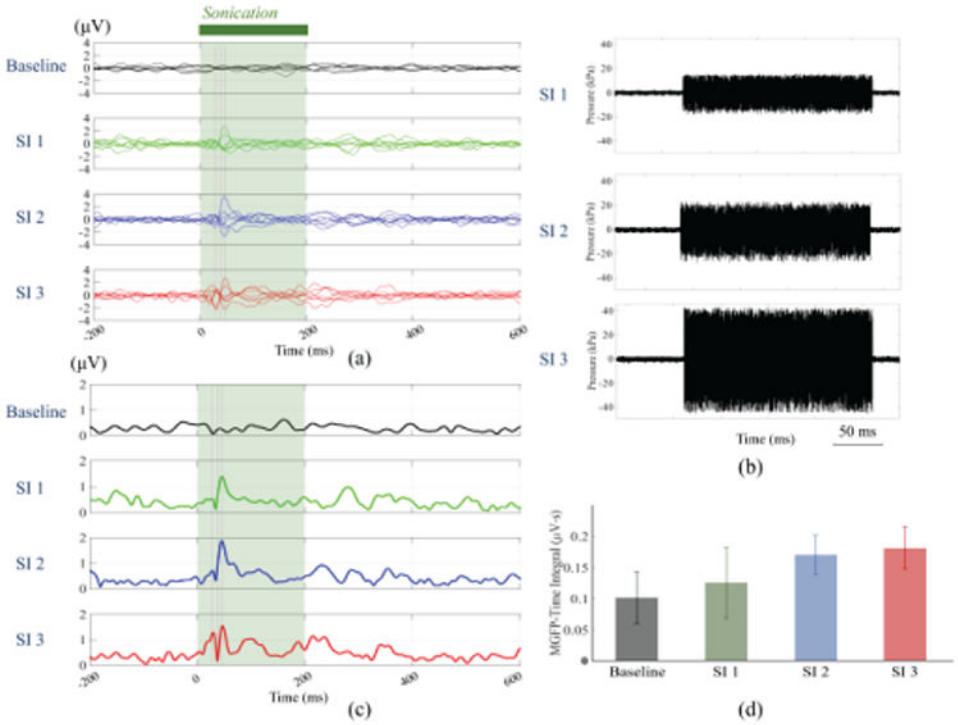

Fig. 2.

tFUS-evoked brain activities induced by three sonication intensities (as shown in Table I) recorded by 8-channel scalp EEG. (a) Butterfly plots of EEG waveforms, (b) ultrasound pressure-time plots for each sonication intensity, (c) EEG MGFP plots, and (d) a bar plot of averages of MGFP-time integral values with standard deviations among trials.

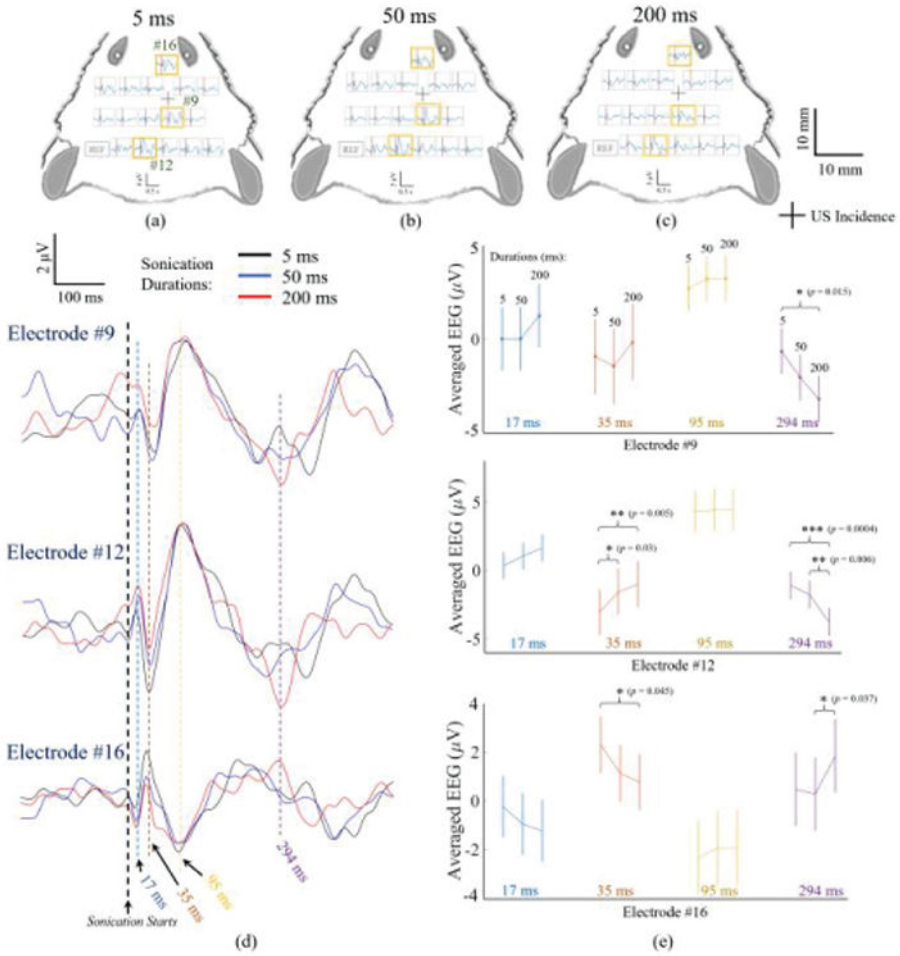

Fig. 3.

Averages of ultrasound-induced electrical potentials recorded with a 16-channel EEG in response to (a) 5 ms, (b) 50 ms, and (c) 200 ms sonication conditions in a top-view of the rat head. The channels indicated by the orange squares, i.e. electrode #9, #12, and #16 are shown at a higher gain in (d), in which the EEG recordings with three sonication durations are plotted for each electrode. The vertical dotted lines demonstrate the time points (17, 35, 95 and 294 ms) of interests at which the peaks of neural activity locate, and those average values and standard deviations are depicted in (e). The t-tests with p values indicate significant effects of sonication durations in each electrode as presented in (e).

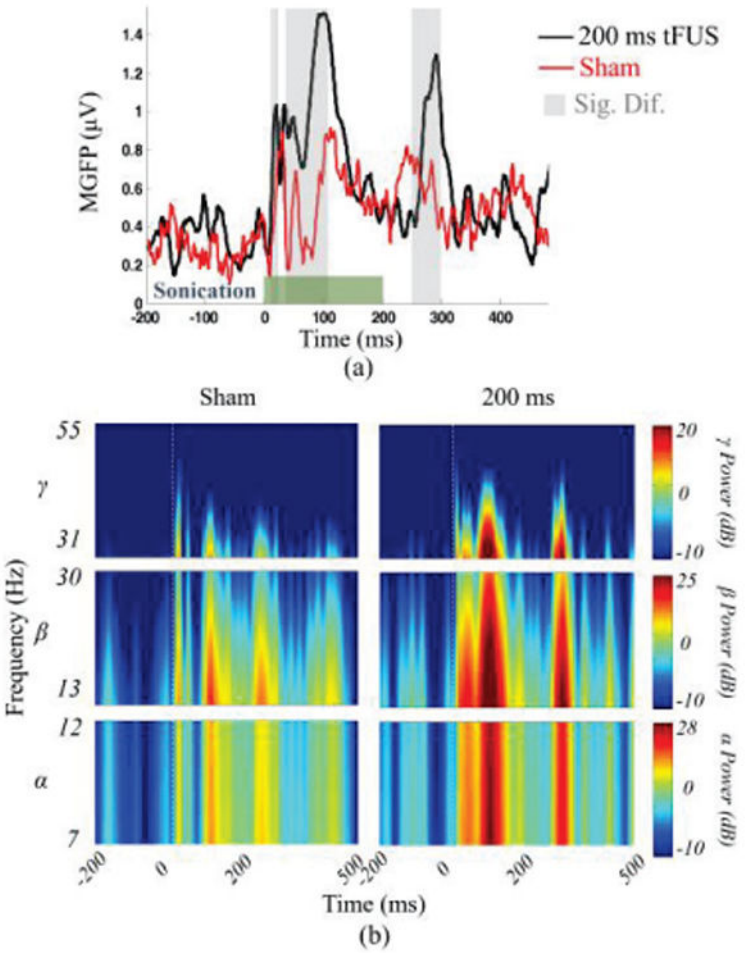

Fig. 4.

Comparing the brain activity during sonication with the sham condition. (a) The MGFP is depicted for the two conditions, namely the 200 ms sonication (I_{spta}: 0.6 mW/cm^2, I_{sppa}: 4.6 mW/cm^2, I_{sptp}: 252 mW/cm^2) and sham. The green bar indicates the duration for which the tFUS was administered (200 ms) and the gray bars indicate the time intervals during which the amplitude of the EEG signal was statistically different for the two conditions ($p<0.025$). (b) The short-time Fourier transform of the MGFP of the two conditions is calculated and compared against each other.

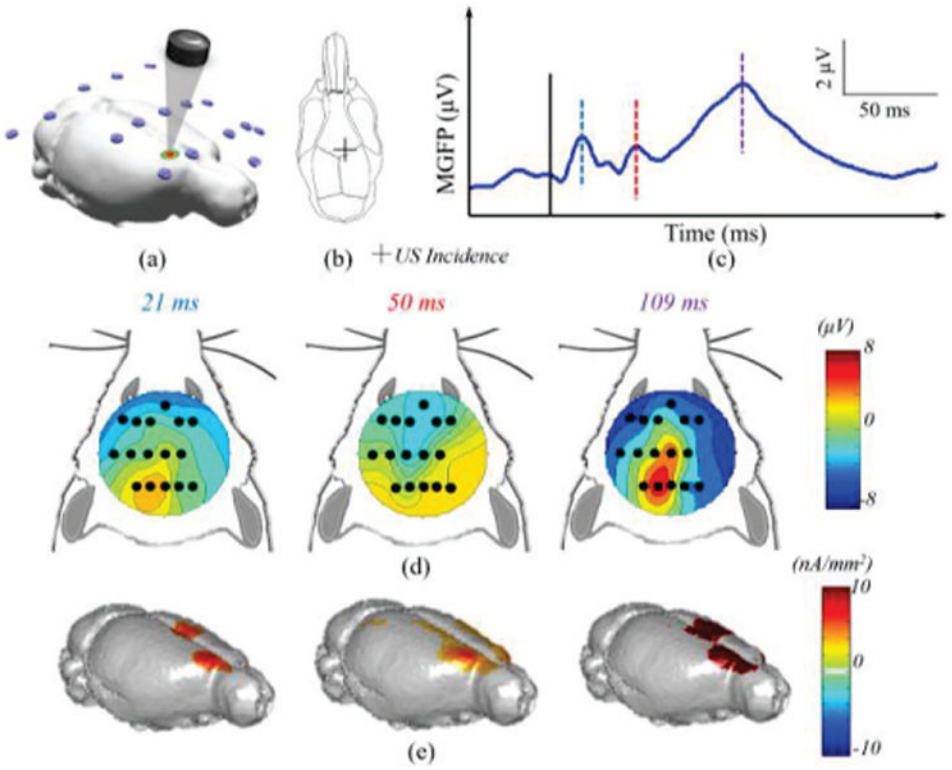

Fig. 5.

ESI neuroimaging of brain activity induced by the 200 ms low-intensity tFUS stimulation at the right anterior cortex in a rat. In this experiment, the tFUS transducer was placed over the right hemisphere as indicated in the 3D model (a), and the schematic diagram (b), where the cross depicts the placement of ultrasound transducer. The MGFP of the recorded EEG signal (c), in which the black solid line indicates the onset of sonication, and the blue, red and purple dashed lines represent the temporal instances of relative peaks in the MGFP (21 ms, 50 ms, and 109 ms). The topographical voltage maps (d) and source images (e) of these instances are depicted correspondingly.

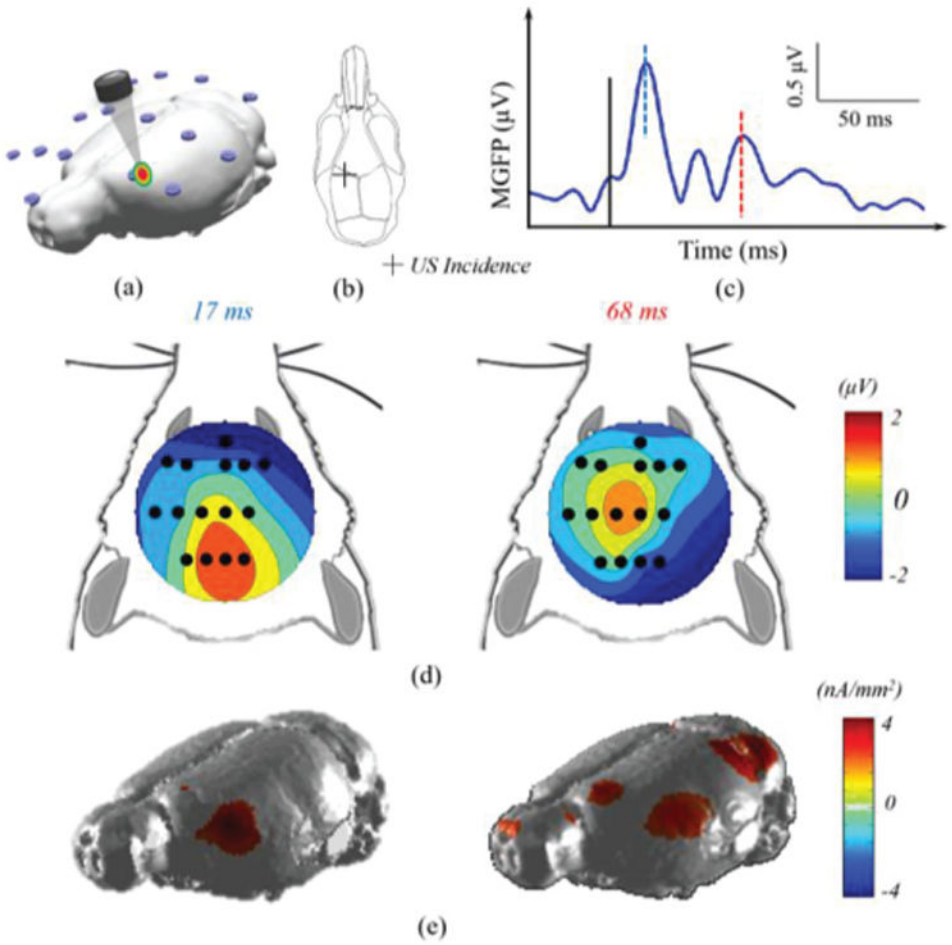

Fig. 6.

ESI neuroimaging of brain activity induced by the 200 ms low-intensity tFUS stimulation at the left anterior cortex of a rat. In this experiment, the tFUS transducer was placed over the left hemisphere as indicated in the 3D model (a) and the schematic diagram (b), where the cross depicts the placement of ultrasound transducer. The MGFP of the recorded EEG signal (c), in which the black solid line indicated the onset of sonication, and the blue and red dashed lines points to the temporal instances of the relative peaks in the MGFP (17 ms, and 68 ms). The topographical voltage maps (d) and source images (e) of these instances are depicted correspondingly.

Table 1

Ultrasound Parameters for three sonication Intensities (SI)

Parameters	SI 1	SI 2	SI 3
I_{spta} (mW/cm^2)	0.1	0.2	0.6
I_{sppa} (mW/cm^2)	0.7	1.4	4.6
I_{sptp} (mW/cm^2)	38	83	252
P_r (kPa)	18.3	27.9	45.9
P_p (kPa) [a]	16.1	22.8	42.8

[a] P_p: spatial-peak positive pressure amplitude.